

Application of TiC reinforced Fe-based coatings by means of High Velocity Air Fuel Spraying

K Bobzin, M Öte, M A Knoch, X Liao and J Sommer

Institut für Oberflächentechnik, RWTH Aachen University, Germany

E-Mail: sommer@iot.rwth-aachen.de

Abstract. In the field of hydraulic applications, different development trends can cause problems for coatings currently used as wear and corrosion protection for piston rods. Aqueous hydraulic fluids and rising raw material prices necessitate the search for alternatives to conventional coatings like galvanic hard chrome or High Velocity Oxygen Fuel (HVOF)-sprayed WC/Co coatings.

In a previous study, Fe/TiC coatings sprayed by a HVOF-process, were identified to be promising coating systems for wear and corrosion protection in hydraulic systems. In this feasibility study, the novel High Velocity Air Fuel (HVOF)-process, a modification of the HVOF-process, is investigated using the same feedstock material, which means the powder is not optimized for the HVOF-process. The asserted benefits of the HVOF-process are higher particle velocities and lower process temperatures, which can result in a lower porosity and oxidation of the coating. Further benefits of the HVOF process are claimed to be lower process costs and higher deposition rates. In this study, the focus is set on to the applicability of Fe/TiC coatings by HVOF in general. The Fe/TiC HVOF coating could be produced, successfully. The HVOF- and HVOF-coatings, produced with the same powder, were investigated using micro-hardness, porosity, wear and corrosion tests. A similar wear coefficient and micro-hardness for both processes could be achieved. Furthermore the propane/hydrogen proportion of the HVOF process and its influence on the coating thickness and the porosity was investigated.

1. Introduction

An important point for components in hydraulic applications is their lifetime. In the hydraulic steelwork, a lifetime of 30-50 years is a common demand [1]. To fulfil this requirement, the used piston rod has to be protected against wear and corrosion. Typical coatings for highly loaded hydraulic components are WC/CoCr and Cr₃C₂/NiCr sprayed by HVOF. These coatings exhibit a good corrosion and wear protection. Raw material prices have, however, risen over the last years. Therefore, researchers and the industry are investigating possible alternative cost efficient systems with comparable resistance to mechanical and corrosive attack. One alternative is the reduction of the carbide content of the coating. Another alternative is to investigate cost-efficient and ecological [2] Fe-based matrix materials with alternative hard materials, like TiC. Moreover, it can be noted that the additives in lubricants are often optimized for Fe-based materials, in order to increase the corrosion protection of the technical components [3].

In a previous study of the authors, TiC reinforced Fe-based (Fe/TiC) coatings with a relatively low carbide content (34 wt.-%) has been developed considering the above-mentioned issues. Fe/TiC coatings were applied on the carbon steel C45 using two different HVOF systems; one operated with liquid fuel and one operated with gaseous fuel. Electroplated hard chrome and WC/CoCr HVOF



coatings were used as references. The corrosion properties of the coatings system were investigated using polarization tests in artificial sea water (ASW) and in two typical flame retardant hydraulic lubricants. The wear properties were tested using a linearly reciprocating tribometer. In both the corrosion and wear tests, the Fe/TiC coatings showed similar or even better behaviour than the references. Of particular note is that the TiC in the Fe/TiC coating was partially converted into TiO_2 . It was furthermore observed that Cr reacted with C and formed Cr_3C_2 . A partial oxidation of matrix material was observed as well. The results show that HVOF sprayed Fe/TiC coatings can be used as an alternative coating system for protecting highly loaded piston rods in marine environments. [4]

The HVOF process is a modification of the HVOF process [5]. Compared to a HVOF process, the HVAF process has some different characteristics, e.g. a lower process temperature. The lower process temperature is achieved by using air instead of oxygen as oxidant [5]. The lower combustion temperature can result in coatings with a lower content of oxides. A number of studies confirm this hypothesis [5, 6, 7, 8, 9, 10]. The variety of different torch designs must, however, not be neglected in this consideration. Thus, no general statement concerning the oxygen content of HVOF and HVAF coating can be made [7]. In [11], HVAF WC/Co(Cr) coatings showed less oxidized phases and the amount of dissolved cemented carbides was lower, in comparison to HVOF coatings. This effect is ascribed to the lower combustion temperature. The gas flow rates in HVAF are higher than the one in HVOF. This can, in turn, enable a higher powder mass flow rate and consequently higher deposition rates [12]. The coating quality of coatings produced using parameters optimized for high deposition rates have yet to be investigated.

As stated in [4], using the HVOF process for applying Fe/TiC coatings, the following reactions took place. The TiC particles of the powder were partially converted into TiO_2 phases in the coating and the Cr parts of the powder reacted with C and formed Cr_3C_2 in the coating. With the assumption that, these reactions can be influenced by the combustion temperature, the idea of this study was to use the HVAF process to deposit Fe/TiC coatings. In this study, the focus lies on the feasibility of producing such HVAF Fe/TiC coatings. Here it must be noted that the powder fraction was not optimized for the HVAF process. To the knowledge of the authors, the applicability of Fe/TiC coatings by means of HVAF process and the corrosion and wear protection of these coatings applied with this technology have not been investigated in the literature, yet.

2. Experimental setup and description

The behaviour of coatings applied by means of HVOF and HVAF under corrosive and tribological loading was investigated using electro-chemical corrosion tests and a PoD tribometer. The coatings were investigated metallographically in the as-sprayed state and after the corrosion tests. Furthermore, the coatings' microhardness was measured. Before the microhardness measurements, the electro-chemical corrosion and the PoD tests, the coated samples were ground and polished to a surface parameter $R_z \approx 3 \mu\text{m}$.

1.0503 (C45) is a typical piston rod material and is, therefore, used as substrate material. The samples have the dimensions $50 \times 30 \times 8 \text{ mm}^3$. An iron-based matrix (51.5 wt.-% Fe, 27 wt.-% Cr, 18 wt.-% Ni and 3 wt.-% Mo) and 34 wt.-% of TiC was used as feedstock material. Quite high Cr and Ni contents were chosen to ensure a good corrosion resistance of the coating. The powder was agglomerated and sintered with a grain size fraction of $-45 + 10 \mu\text{m}$ (Oerlikon Metco WOKA GmbH, Barchfeld, Germany). The agglomerates have a spherical shape. The TiC particles have an average size of approximately $2 \mu\text{m}$ and are evenly distributed in the powder. For both the HVOF and the HVAF process, the same feedstock material was used.

The HVAF coatings were produced using an AK-07 system (Kermetico Inc., Benicia, USA). The first attempts did, however, clog the nozzle. To avoid the clogging, the propane flow rate was set at minimum and the air flow rate at maximum. This parameter set can be designated "cold" and, therefore, the particles exhibit relatively low temperatures resulting in reduction in nozzle clogging. This parameter set is called "HVAF 1". The SEM-image of parameter set "HVAF 1" shows a high porosity, which may be unfavourable for the use as a corrosion protection coating. To produce denser

coatings, the temperatures of the sprayed particles need to be increased, which would influence flattening behaviour of the feedstock material. Two strategies for changing the flattening behaviour were used. The first strategy was to increase the propane gas flow rate and the second was to add hydrogen into the combustion chamber, additionally. If the propane flow rate is increased, the combustion temperature increases. If a hydrogen flow rate is added into the combustion chamber, the heat transfer between the spray particles and the gas-mixture is improved [13]. For both mechanisms, stable process parameters could be identified. In the following, one sample each for both mechanisms will be presented in addition to sample HVAF 1. The samples are named HVAF 2 and HVAF 3. The selection was based on the achieved porosity and the wear and corrosion behaviour. For the sake of completeness, all process parameters are given in table 1.

Table 1. HVAF-Spray parameters for the AK-07.

Constant Parameter	Value	Sample Name	Propane Pressure (bar)	Hydrogen (SLPM)	Stand-off distance (mm)
Nitrogen flow rate	19 SLPM	HVAF 1 (Ref.)	5.5	0	175
Powder feed rate	40 g/min	HVAF 2 (P1.1)	5.8	0	175
Air pressure	7.3 bar	(P1.2)	5.8	0	210
		(P2)	6.1	0	175
		(H1)	5.5	2.5	175
		(H2)	5.5	5	175
		(H3)	5.5	10	175
		HVAF 3 (H4)	5.5	15	175
		(H5)	5.5	20	175

In order to assess the microstructure, cross sections of the HVAF coatings were prepared. The cross section were analysed using scanning electron microscopy (SEM; LEO 1530 VP Gemini, Carl Zeiss AG Microscopy, Oberkochen, Germany) and energy dispersive X-ray spectroscopy (EDS; Quantax 200 from Bruker Nano GmbH, Berlin, Germany). The porosity of the coating was determined with the evaluation software Image Analysis and a light microscope Zeiss Axiophot (both Carl Zeiss AH, Oberkochen, Germany).

The microhardness of the coatings was measured with the measurement system; Micromet 1 (Buehler, Illinois, USA). For this purpose, the coating was loaded with a weight of $m = 300$ g for $t = 15$ sec. Every coating of each parameter set was measured 10 times in order to generate statistically relevant data.

As stated in the introduction, in a previous study by the authors, Fe/TiC HVOF coatings were investigated [4]. In this study, the best corrosion and wear properties could be achieved using the parameter set shown in table 2 using a K2 HVOF torch (GTV Verschleißschutz GmbH, Luckenbach, Germany).

Table 2. Spray parameters for the K2 [4].

Parameter	Value
O ₂ flow rate	870 SLPM
Kerosene L/h	20 L/h
Oxygen/Fuel ratio λ	1.4
Stand-off distance	300 mm
Transversal Speed	1,000 mm/s
Powder feed rate	29 g/min

For the investigation of the wear properties, a Pin-on-Disc (PoD) tribometer (CSM Instruments SA, Freiburg, Germany) was used. An Al₂O₃ ball with a diameter $\phi = 6$ mm was used as counter body.

Al₂O₃ was chosen to characterise the wear properties of the coatings. The use of Al₂O₃ counter body material ensures the comparability as Al₂O₃ is widely used for wear tests. For more application oriented tests, the counter body material should be changed, e.g. to the seal material. The further PoD parameters are shown in table 3. The 15 x 15 mm² samples were tested using a hydrofluorocarbon (HFC) lubricant as well as without a lubricant. The experiments with lubricant were done to investigate the influence of a typical hydraulic fluid used in low flammability applications. The HFC lubricant was provided by Fuchs Hydraulik GmbH & Co. KG (Kirn, Germany), the exact composition is confidential. Subsequent the wear test, the wear coefficient K for the samples was determined using equation (1) [2]. Therefore, the volumetric wear V and the measured wear track diameter d_t was determined using confocal laser scanning microscopy (VKX 200, Keyence Corporation, Osaka, Japan).

Table 3. PoD test parameters.

Parameter	Value
Wear track diameter d	5 mm
Wear track length s	500 m
Normal load w	10 N
Rotation speed	10 cm/s
Test temperature	RT

$$K \left[\frac{\text{mm}^3}{\text{Nm}} \right] = V \cdot \left[w \left(s \cdot \frac{s}{d_t} \right) \right]^{-1} \quad (1)$$

To analyse the corrosion resistance of the samples, polarization tests were performed in ASW at room temperature in accordance to DIN 50905-4. ASW is an electrolyte, which simulates the real environment in marine applications while maintaining the comparability. Therefore, ASW is important for testing coatings used in coastal areas and offshore constructions. A Calomel-(Hg₂Cl₂) electrode was used as reference electrode and the potential scan rate was set at 0.5 mV/s. The rest potentials and the corrosion current densities were investigated using the Tafel slope analysis.

3. Results and discussion

Figure 1 shows a selection of SEM images of the HVAF coatings. All coatings HVAF 1, HVAF 2 and HVAF 3 exhibit a good bonding to the substrate. The coating thickness d_{ct} of the samples was measured at d_{ct} = 232 – 296 µm. Coating thicknesses differ significantly from each other, although all samples were sprayed with the same number of passes and the same robot parameters. The sample HVAF 1 exhibits the biggest area with local inhomogeneities, like porosity and imperfections. The magnification of HVAF 1 shows a high porosity area near the substrate. To minimize the porosity, the parameters were varied as described in chapter “2. Experimental setup and description”. The sample HVAF 2 was sprayed with a higher propane flow rate to increase the temperature in the combustion chamber. In general, this coating shows significantly less local inhomogeneities than the sample HVAF 1. The measured porosity of this sample was 1.9 %. In the high magnification view of sample HVAF 2, some small pores can be seen, especially in the top layers. These small pores can be assumed to be the result of a reduced compression of the coating applied during the last passes. For the following corrosion and wear tests, the samples were polished. Thus, the small pores in the top layer will not influence the corrosion tests. Such a finishing is common practice throughout the industry and therefore, the increased inhomogeneity displayed in the magnification is assumed to be irrelevant. Generally speaking, this sample shows a much denser coating than the sample HVAF 1. For sample HVAF 3, the hydrogen flow rate was increased in order to increase the heat transfer between the particles and the gas flow. The cross section of this coating shows a dense coating. In high magnification view, one unmolten particle can be seen. The porosity of this coating was about 2.6 %.

Areas with local inhomogeneities were not detected for sample HVAF 3. In conclusion, the local inhomogeneities of the coating could be decreased by increasing the propane gas flow rate and adding a hydrogen gas flow.

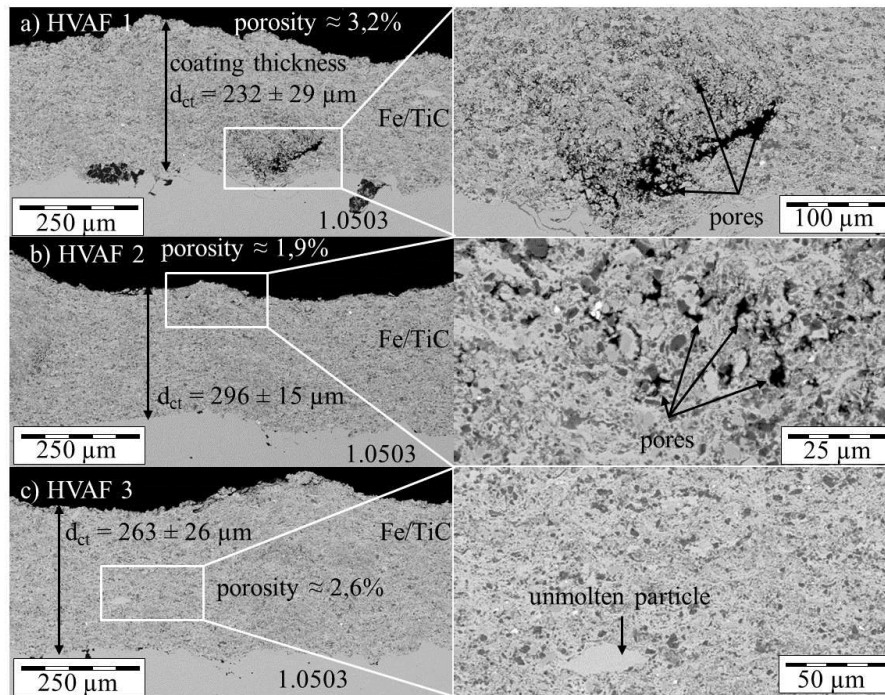


Figure 1. SEM images of the samples HVAF 1 (a), HVAF 2 (b) and HVAF 3 (c).

In figure 2, the SEM images as well as the results of the EDS analysis of the coatings HVAF 1 and HVAF 2 are shown. In the coatings, Cr carbides, Ti carbides, mixed oxide phases and a solid solution were detected. The solid solution consists of Cr, Fe, Ni and Mo. The mixed oxide phases have a high content of Ti. An explanation for the oxidized matrix parts with a high Ti content might be decarburisation and the high kinetic energy of the TiC particles. If the TiC particles hit the surface, they can break brittlely, react with the air and phases with a high TiO_2 content can form. In the sample HVAF 1, an additional Mo phase could be detected.

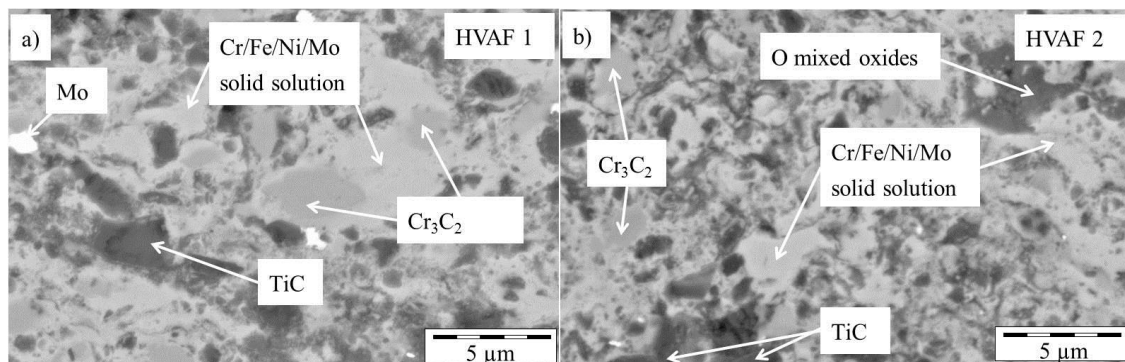


Figure 2. SEM/EDS analysis of the sample HVAF 1 (a) and HVAF 2 (b).

In figure 3 the microhardnesses of the considered samples are shown. Ten measurements were conducted for every sample. All HVAF coatings have a much higher hardness than the substrate. The

sample HVAF 1 shows the lowest microhardness of 630 HV0.3. The microhardness of sample HVAF 3 has a value of 672 HV0.3. The samples HVAF 2 and HVOF show a similar microhardness of 694 HV0.3 and 730 HV0.3. The lower microhardness of the samples HVAF 1 and HVAF 3 is assumed to be a result of the higher porosity of these coatings compared to that of the other coatings HVAF 2 and HVOF. It can be noted that a lower microhardness was measured for samples, which have a higher porosity. The sample HVOF has a porosity about 1 %. All HVOF and HVAF samples have a high standard deviation with regard to their microhardness, which is typical for thermally sprayed coatings. This means the microhardness of the coatings varies, depending on the position of the indentation.

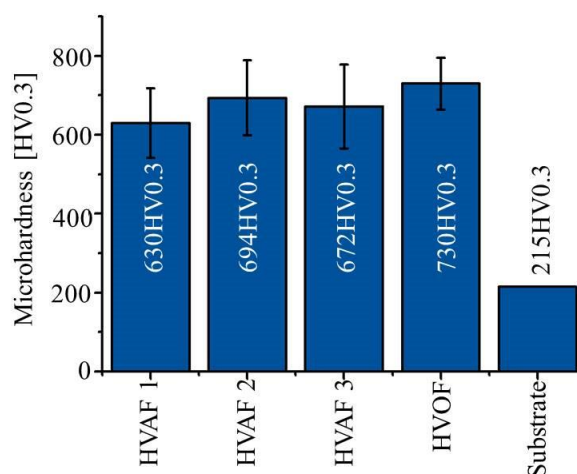


Figure 3. Microhardness of the samples HVAF 1, HVAF 2, HVAF 3, HVOF and the substrate.

In figure 4 the polarization curves of the coatings and the uncoated substrate material in ASW are shown. The rest potential (U_R) and the corrosion current density (i_c) of the samples are shown in table 4. In ASW, the substrate has the lowest corrosion resistance. It has the lowest rest potential with a value of $U_R = -457 \text{ mV}_H$ and the highest corrosion current density of $i_c = 0.0096 \text{ mA/cm}^2$. The curves of the HVOF and the HVAF Fe/TiC coatings are comparable. Among these, the rest potential of the coating HVAF 3 is the highest, meaning it is the noblest coating, whereas the HVOF coating is the least noble one. The HVOF coating has the lowest corrosion current density, whereas the coatings HVAF 2 and HVAF 3 show a slightly higher corrosion current density. The sample HVAF 1 shows the highest corrosion current density of all coated samples. An interesting aspect can be found for sample HVAF 2, which has the lowest current density until the breakthrough at about $U = 100 \text{ mV}_H$. Within the potential range of $U = 400 - 550 \text{ mV}_H$, HVAF 1 and HVAF 2 have almost identical current densities as the substrate. For higher overpotentials, a slight drop can be seen for both samples. Over a large area, the corrosion rates of the coatings HVAF 2 and HVAF 1 is significantly smaller than the rate of the substrate. The samples HVAF 3 and HVOF did not exceed the current density of the substrate. It should be noted that this behaviour can only be detected after the breakthrough. Since there are many unknown factors, which may influence the current density in this area, e.g. the temperature, electrolyte aging, etc. closer attention should be paid to the area before the breakthrough potential. It should be noted that the HVOF sample exhibits lower current densities after the breakthrough and thus, the overall corrosion rate after the polarization test is assumed to be lower for the HVOF sample. As a result of the corrosion tests, it can be stated that the coating HVAF 2 shows the lowest corrosion rates of all samples until the breakthrough. The results of the polarization curves can be summarized as followed. The HVAF coatings have the highest rest potential and, until the breakthrough, these coatings show similar or even better corrosion behaviour than the HVOF coating.

Sample HVAF 2 has the lowest porosity and overall the lowest current density of all HVAF coatings. Despite the high overpotential of $\Delta U > 1.25$ V, all coatings show a lower corrosion rate than the substrate. This clearly indicates that all coatings protect the substrate during the entire corrosion test.

Table 4. Current density curves data.

Sample	Rest potential U_R [mV]	Corrosion current density i_c [mA/cm ²]
Substrate	-457	0.0096
HVAF 1	-316	0.0050
HVAF 2	-300	0.0022
HVAF 3	-286	0.0035
HVOF	-360	0.0014

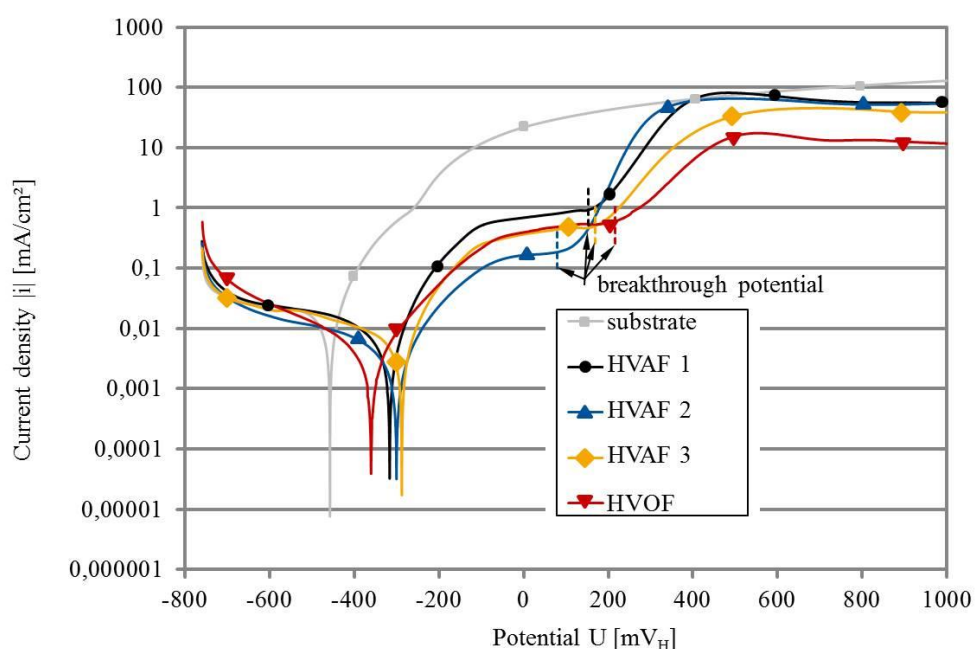


Figure 4. Corrosion current potential curves of the coatings in ASW at RT.

In figure 5, cross sections of the samples HVOF, HVAF 1, HVAF2 and HVAF 3 after the corrosion tests are shown. The cross sections confirm the results of the polarization test. For all samples, it can be seen that there was no corrosion of the substrate. The oxidation of the matrix is more distinct for the HVAF than the one of the HVOF sample. Consequently, the HVOF coating has a bigger remaining thickness of uncorroded coating material than the HVAF coatings. This corrosion behaviour can be traced to the lower overall current density of the HVOF sample.

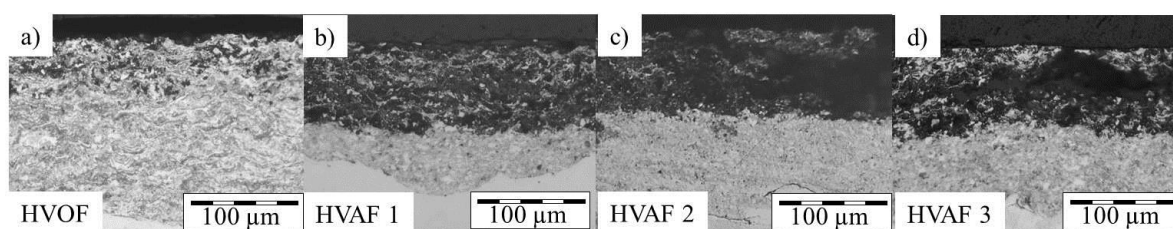


Figure 5. Cross-section polishes of the samples HVOF (a), HVAF 1 (b), HVAF 2 (c) and HVAF 3 (d). In figure 6, the results of the POD tests are shown. In figure 6 a), the wear tracks for the samples HVAF 2 and HVAF 3 are displayed. The images of the unlubricated wear tracks show non-homogeneous wear tracks with similar characteristics for all HVOF and HVAF coatings. All samples have abrasive wear behaviour and splat breakages. The samples HVOF and HVAF 3 exhibit qualitatively less outbreaks than the sample HVAF 2. A high porosity of the coating promotes breakages of the coating, which correlates with the images shown in Figure 6. The porosity offers a target for the counter body and a chunk of the coating can break out. For the lubricated tests, wear tracks with homogeneous shape and no significant outbreaks were detected.

In figure 6 b), the wear coefficient K for the unlubricated and the lubricated wear tracks is shown. All coatings show a lower wear rate than the substrate. This applies to the unlubricated and lubricated experiments. For the unlubricated coatings, the sample HVAF 1 shows the highest wear coefficient of $K = 2.7 \cdot 10^{-5} \text{ mm}^3/\text{Nm}$. With the parameter set HVAF 3, a similar wear coefficient $K = 1.4 \cdot 10^{-5}$ as for the HVOF sample was achieved. In general, the lubricated wear coefficients K are much lower than the unlubricated ones. The highest wear coefficient K was again measured for the substrate. The sample HVAF 1 achieved a wear coefficient of $K = 2.1 \cdot 10^{-6} \text{ mm}^3/\text{Nm}$. The lowest wear coefficient K was achieved for the sample HVOF 3 with a value of $K = 5.2 \cdot 10^{-7} \text{ mm}^3/\text{Nm}$. For the HVOF sample, the lubricated wear could not be determined due to an instrumental failure. The images of the wear tracks and the detected wear coefficient K correlate. The sample with the lowest wear has the lowest amount of outbreaks.

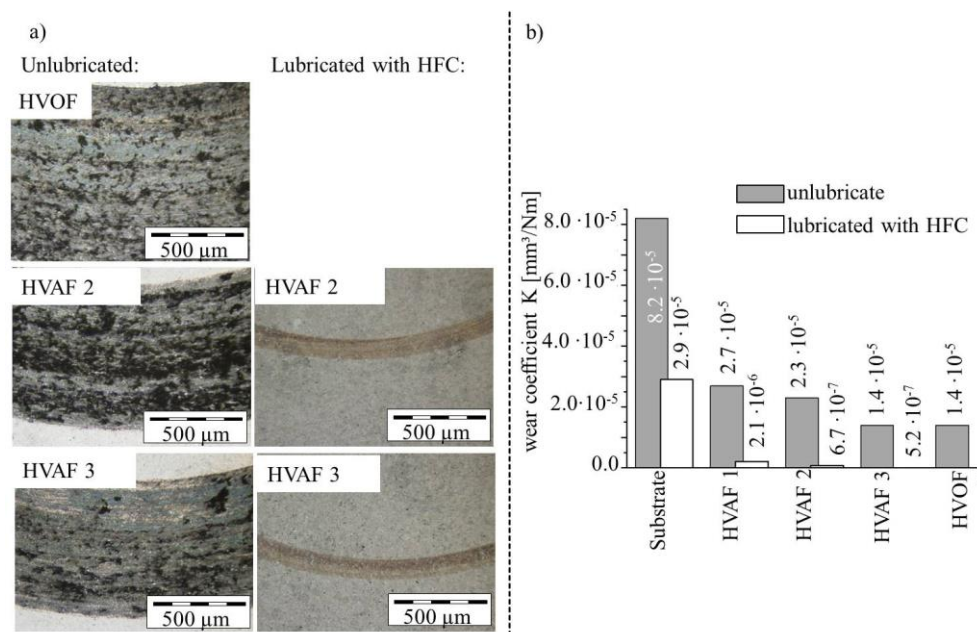


Figure 6. Wear tracks of sample HVOF, HVAF 2 and HVAF 3, (a) Wear of friction without lubrication and with lubrication (b).

4. Conclusion and outlook

The aim of this study was to proof the feasibility of applying Fe/TiC coatings using the HVAF process. Fe/TiC coatings were successfully applied onto a 1.0503 substrate. The first set of parameter shows larger areas with inhomogeneities. After a parameter variation, these inhomogeneities could be reduced. In the EDS analysis, mixed oxides could be detected in the HVAF coatings. In a further study, the oxide percentage of the HVAF and HVOF coatings can be compared as this might explain the differences in the corrosion and wear behaviour. All HVAF coatings achieve a better wear behaviour than the substrate in lubricated and unlubricated tests. The corrosion behaviour of all

coatings is better than that of the substrate. Furthermore, similar trends can be observed for moderate overpotentials for all coatings. Nonetheless, the differences in the polarization curves clearly show that the process parameters are an important factor. For low overpotentials, the coating HVOF 2 shows the best corrosion behaviour of all coating systems until the breakthrough. This coating does also exhibit the lowest porosity of all HVOF coatings indicating the porosity influences the corrosion behaviour and that lower porosity is favourable. The broad range of the feedstock material's grain size is assumed to be one reason for the uncharacteristically high porosity of all HVOF coatings. For a further coating optimization, it could therefore be useful to use powders with a narrower grain size than the one used in this study. Another aspect which may consider is the optimization of the HVOF torch. To avoid nozzle clogging, a smaller combustion chamber and smaller nozzles can be used.

Acknowledgments

This work is based on the DFG project BO 1979/45-1. The authors gratefully acknowledge the financial support of the German Research Foundation (DFG).

References

- [1] Burhart H F 2011 Kolbenbeschichtung, Verfahren, Qualitätsbeurteilung und Trends *IFAS-Kolloquium, Aachen Germany*
- [2] Milanti A, Koivuluoto H, Vuoristo P and Bolelli G 2014 Microstructural characteristics and tribological behavior of HVOF-Sprayed novel Fe-based alloy coatings *Coatings* **4**
- [3] Findeisen D and Feldhuser S 2015 *Ölhydraulik* (Berlin: Springer)
- [4] Bobzin K, Öte M, Linke T F and Malik, K A 2016 Wear and corrosion resistance of Fe-based coatings reinforced by TiC particles for application in hydraulic systems *Journal of Thermal Spray Technology* **25** pp. 365-74
- [5] Guo R Q, Zhang C, Chen Q and Yang Y 2011 Study of structure and corrosion resistance of Fe-based amorphous coatings prepared by HVOF and HVOF *Corrosion Science* **53** 2351-56
- [6] Wang Q, Zhang S, Cheng Y and Xiang J 2013 Wear and corrosion performance of WC-10Co4Cr coatings deposited by different HVOF and HVOF spraying processes *Surface & Coating Technology* **218** pp. 127-36
- [7] Bolelli G, Berger L M, Boerner T and Koivuluoto H 2015 Tribology of HVOF- and HVOF-sprayed WC-10Co4Cr hardmetal coatings: a comparative assessment *Surface & Coating Technology* **265** 125-44
- [8] Hulka I, Serban V A, Niemi K and Vuoristo P 2012 Comparison of structure and wear properties of fine-structured WC-CoCr coatings deposited by HVOF and HVOF spraying Processes *Solid State Phenomena* **188** 422-27
- [9] Bolelli G, Hulka I, Koivuluoto H and Lusvarghi L 2014 Properties of WC-FeCrAl coatings manufactured by different high velocity thermal spray processes *Surface & Coating Technology* **247** 74-89
- [10] Berger L M, Puschmann R, Spatzier J and Matthews S 2013 Potential von HVOF-Spritzprozessen *Thermal Spray Bulletin* 17-20
- [11] Hashmi S 2014 Comprehensive materials processing: thermal spray coating process *Newnes* 230-266
- [12] Salman A, Gabbitas B, Cao P and Zhang D 2009 Tribological properties of Ti(AlO/Al₂O₃) composite coating by thermal spraying *International Journal of Modern Physics* **23** 1407-12
- [13] Verstak A and Baranovski V 2006 AC-HVOF sprayed tungsten carbide: properties and application *Proc. ITSC Seattle, USA*